Received: 11 March 2022 | Revised: 28 April 2022 | Accepted: 5 May 2022 | Published on: 21 June 2022

DOI: 10.1002/asna.20220018

Astronomische Nachrichten

REVIEW ARTICLE

Rectilinear elements of visual optical double stars: With application to the 1829 southern double star catalogue of James Dunlop

Roderick R. Letchford | **Graeme L. White** | **Carolyn J. Brown**

Centre for Astrophysics, University of Southern Queensland, Toowoomba, Queensland, Australia

Correspondence
Roderick R. Letchford, Centre for Astrophysics, University of Southern Queensland, Toowoomba 4350, QLD, Australia.
Email: rod.letchford@usq.edu.au

Abstract

The relative Rectilinear motion of optical double stars provides an important clue to the relationship of the components. We provide an objective method of confirming the optical status of double stars, and of obtaining unbiased rectilinear elements solely on data obtained from the HIPPARCOS and *Gaia DR2* space missions. We apply this technique to determine the rectilinear elements of 14 optical double stars from the southern double star catalogue of James Dunlop. The resultant uncertainties are, on average, an order of magnitude smaller than the method currently used.

KEYWORDS

astrometry, binaries: visual, celestial mechanics, stars: kinematics

1 | INTRODUCTION

Distinguishing between optical and binary double stars has important ramifications for many aspects of astrophysics (Letchford et al. 2022b, paper II). The rectilinear elements of optical double stars describe the on-sky projection of the linear motion of the secondary star compared with the primary. The *United States Naval Observatory* (USNO) maintains the *Second Catalogue of Rectilinear Elements* (Hartkopf & Mason 2020), hereafter referred to as the SCORE, which contains the rectilinear elements of over 1,200 double stars, determined from historic astrometric measures with typical uncertainties of ∼0.2 arcseconds (″), and uncertainties in average relative proper motion of ∼3 milli-arcseconds per year (mas year^{-1}).

The first attempt to describe the relative linear motion of an optical double star was by Schlesinger & Alter (1912) (they provide no references to earlier work), who used a least squares method on historic measures after precession to a common equinox. This method was later adopted by Torres (1985, 1988a, 1988b). Debehogne & de Freitas Mourao (1977) who undertook a comparison between the least squares method and that of mean places with differential corrections, opted for the least squares method as the best. Equations for the least squares method can be found in Torres (1988b). The SCORE rectilinear elements result from the least squares method applied to *weighted* historic measures, where weighting is described in Hartkopf et al. (2001) and Mason et al. (1999).

Rectilinear plot visualization (and rectilinear elements) has a number of important benefits. Any erroneous, or poor measures, are readily identified and non-linear motion resulting from orbital motion of a binary system is easily visualized by curvature in the linear path of the companion, as are nonlinear sub-motions due

to close additional components such as astrometric binaries (Hartkopf & Mason 2020). In addition, well-defined linear elements provide scale calibration for imaging systems and proper motions comparable in precision with those of HIPPARCOS (Perryman et al. 1997) and *Gaia DR2* (Gaia Collaboration et al. 2018).

The aim of this paper is to present a modified method of obtaining the rectilinear elements of confirmed optical double stars from the space-based astrometry of HIPPARCOS (via ASCC, Kharchenko 2001) and *Gaia DR2* alone, and which relegates historic measures to a secondary role of confirmation of curvature or other nonlinear motion, in the Rectilinear plots. We then apply this method to a set of confirmed optical double stars.

The set of double stars from which we extract a subset of confirmed optical double stars we call the *Working Dunlop Catalogue*, which itself is a subset from the first published catalogue of southern double stars by James Dunlop (Dunlop 1829). This original 1829 catalogue will hereafter be referred to as the *Dunlop Catalogue*. A previous paper by the authors (Letchford et al. 2022a, paper I) described and analyzed the accuracy of the original 1829 *Dunlop Catalogue* based on ASCC and *Gaia DR2* source identifiers (where available). A digitized version is available on the website of paper I under supplementary data.[1] The *Working Dunlop Catalogue* is defined in paper II and is a subset of 40 pairs from the original *Dunlop Catalogue* (of 253 pairs), which have entries in the *The Washington Double Star Catalogue* (WDS, Mason et al. 2001) and for which accurate astrometry is available, both in ASCC and *Gaia DR2*. The *Working Dunlop Catalogue* is thus a reliable and accurate catalogue of pairs with observational histories of ∼200 years.

The first two authors of this paper have earlier published material on the Rectilinear motion of optical double stars (Letchford et al. 2018, 2019). This present paper is a more thorough investigation of Rectilinear motion and presents a modified technique.

Section 2 of this paper summarizes the method used in paper II for the separation of binary and optical double stars, and presents a conservative list of "confirmed" optical double stars from the *Working Dunlop Catalogue*. Section 3 proposes our technique for determining the rectilinear elements of optical double stars and compares the results with rectilinear elements from the SCORE. Section 4 presents and discusses the results of applying our technique to the confirmed optical double stars from the *Working Dunlop Catalogue*.

[1] https://doi.org/10.1093/mnras/stab3777.

TABLE 1 Catalogue numbers from the *Dunlop Catalogue* for the 40 double stars for which binding energies E_{binding} could be calculated

Nos. $E_{\text{binding}} < 0$	Nos. $E_{\text{binding}} > 0$
2 in total	**38 in total**
38, 55	2, 4, 5, 23, 26, 27, 28, 29, 40, 41, 52, 57, 73, 77, 79, 80, 114, 116, 118, 146, 155, 175, 176, 178, 184, 186, 200, 215, 225, 232, 236, 238, 241, 242, 245, 246, 248, 250

2 | METHOD: DETECTING OPTICAL DOUBLE STARS

By definition, binary double stars are double stars whose binding energy (E_{binding}) is less than zero (paper II). Therefore, any double star that is not a binary star, that is, whose binding energy is greater than zero, is unbound and therefore must be an optical double star.

In paper II, we selected a subset of double stars from the *Working Dunlop Catalogue* where binding energies were able to be calculated using data from *Gaia DR2*. On the available data, only two double stars had binding energies <0 and 38 had binding energies > 0. These are reiterated here in Table 1. However, large uncertainties are expected in the estimation of binding energies for individual double stars (paper II, equation 1), due to the inexact nature of calculating stellar masses from luminosity estimates (paper II, equation 2) and estimating physical distances from parallaxes (paper II, equation 3) where even a small inaccuracy in a parallax measure can lead to a large uncertainty in physical separations.

Because of the expected large uncertainties in the calculated E_{binding}, paper II placed a conservative criteria for "confirmed" binary double stars of (a) $E_{\text{binding}} < +1$, (b) a physical separation (D) such that $D - 1\sigma < 1pc$, and (c) which displayed common proper motion (CPM). With these constraints, there are eight "confirmed" binary stars (no. 5, 38, 55, 80, 116, 232, 242, and 245) in the *Working Dunlop Catalogue*.

Conversely, 14 of the 38 double stars with $E_{\text{binding}} > +1$ in Table 1 are now suggested as "confirmed" *optical* double stars since $D - 1\sigma > 1pc$ and since they displayed no CPM (paper II). These 14 double stars are given in Table 2 where Column 1 is the catalogue number of the double star from the original *Dunlop Catalogue* retained in the *Working Dunlop Catalogue* and column 2 is the system identifier from the WDS, underneath which is the Discoverer Code identifying the particular double star within the system, also from the WDS. Columns 3–5 give

TABLE 2 Table of 14 "confirmed" optical double stars from the *Working Dunlop Catalogue*

No.	WDS Discoverer code	$E_{binding}$ $M_\odot$ km^{-2} s^{-2}	D pc	No CPM
4	01388-5327 DUN 4	~2.5	1.83 ± 0.56	✓
28	06240-3642 DUN 28AC	~2,700	47.89 ± 0.83	✓
29	06291-4022 DUN 29	~8,600	160.5 ± 5.9	✓
40	07092-5622 DUN 40	~670	146.2 ± 2.4	✓
73	08562-5532 DUN 73AB	3,400	190 ± 11	✓
79	09336-4945 DUN 79	~4,400	8.0 ± 2.2	✓
146	13493-4031 DUN 146	~360	480 ± 21	✓
155	14077-5341 DUN 155	~36	1200 ± 84	✓
178	15116-4517 DUN 178AC	~3,000	10.5 ± 1.8	✓
184	15263-4252 DUN 184	~50	440 ± 9	✓
200	16225-4355 DUN 200	~550	280 ± 14	✓
225	19124-5148 DUN 225AB	~1,500	510 ± 60	✓
241	22366-3140 DUN 241	~400	255.9 ± 6.5	✓
250	23272-5017 DUN 250	~37,000	890 ± 53	✓

Note: The estimated binding energies ($E_{binding}$) have been rounded to two significant figures.
Abbreviations: CPM, common proper motion; WDS, *Washington Double Star Catalogue*.

the binding energy ($E_{binding}$) in $M_\odot$ km^{-2} s^{-2}, the physical separation of the two components of the optical double star in parsecs (*pc*), and an indication that no CPM is found (no CPM, following the methodology of Hartkopf et al. 2013).

The remaining 18 double stars could not be confirmed as either binary or optical double stars because they failed one or two of the three tests necessary for classification as either a binary *or* an optical double star; they are listed in Table 3.

3 | RECTILINEAR MOTION AND RECTILINEAR ELEMENTS

As mentioned in Section 1, we here determine the rectilinear elements in a relatively simple way. We take advantage of space-based astrometry where the uncertainties in the positions of the two stars are measured in milli-arcseconds (mas) and simply describe the straight line running through the HIPPARCOS and *Gaia DR2* positions. This straight line is better determined, by orders

TABLE 3 List of 18 double stars from the *Working Dunlop Catalogue* which cannot be confirmed as either binary or optical double stars

	Indicators for binary double stars			Indicators for optical double stars		
No.	$E_{\text{binding}} < 1$	$D - 1\sigma < 1$	**CPM**	$E_{\text{binding}} > 1$	$D - 1\sigma > 1$	**No CPM**
2		✓	✓	✓		
23		✓	✓	✓		
26		✓	✓	✓		
27			✓	✓	✓	
41	✓	✓				✓
52		✓	✓	✓		
57		✓		✓		✓
77		✓	✓	✓		
114		✓	✓	✓		
118	✓	✓				✓
175	✓	✓				✓
176		✓	✓	✓		
186			✓	✓	✓	
215			✓	✓	✓	
236			✓	✓	✓	
238		✓		✓		✓
246	✓	✓				✓
248		✓	✓	✓		

Note: For these pairs there is sufficient *Gaia DR2* data to calculate each of the three parameters (E_{binding}, D and common proper motion [CPM]—see text), but they do not pass all three tests necessary for confirmation as either a binary or optical double star.

of magnitude, than a similar projection through historic measures. The rectilinear elements are derived from this straight line. The HIPPARCOS (via ASCC) mission has an epoch of observation of 1991.25 and the *Gaia DR2* mission an epoch of 2015.25, and both are at ICRS (≡ equinox 2000.0).

The formal uncertainty in this definition of the Rectilinear proper-motion vector of the secondary, determined from the HIPPARCOS and *Gaia DR2* astrometry, is dominated by the combination (in quadratic form) of the HIPPARCOS and *Gaia DR2* uncertainties in the positions of both the primary and secondary stars, and the uncertainty in the epochs of the observations (considered here to be of little consequence). These are reflected in the rectilinear elements as listed in Table 6.

Historic measures are not used in this calculation of the rectilinear elements as the uncertainties are orders of magnitude larger than those of the space-based measures. Historic measures, either weighted or unweighted, can be placed into the calculation, and onto the Rectilinear plots, not to strengthen the calculations but rather to confirm the values of the rectilinear elements determined without them. Misalignment of the historic data with the Rectilinear plots, or any other variation from the straight line projection of HIPPARCOS and *Gaia DR2*, will be evidence of orbital motion or some form of third body in the system, assuming of course, that the HIPPARCOS and *Gaia DR2* positions and their proper motions are consistent within their uncertainties.

In addition, we adopt the conventional form of conversion from polar to Cartesian coordinates ($x = \rho\cos(\theta)$, $y = \rho\sin(\theta)$, and define $t0$ ($T0$ in the SCORE) to be precisely 2000.0 in every case.

The seven rectilinear elements, with our definitions, are given in Table 4 along with their uncertainties. Derivations of the Cartesian coordinates of the HIPPARCOS and *Gaia DR2* positions and their uncertainties are given in Appendix A (together with the definition of arctan2) and Appendix B, respectively. Formulae for an ephemeris are given in Table 5.

3.1 | Test optical double stars

Any modified method of computing rectilinear elements must be proven with respect to existing methods. A total

TABLE 4 Definition of the rectilinear elements proposed in this paper

Element	Units	Description	Definition	Uncertainty
$x0$	as	Difference in declination (primary – secondary) at time $t0$	$xg - xa(2015.5 - t0)$	$\sigma_{x0} = \pm\sqrt{[(2015.5 - t0)\sigma_{xa}]^2 + \sigma_{xg}^2}$
xa	as year^{-1}	Rate of change of declination	$(xg - xh)/(2015.5 - 1991.25)$	$\sigma_{xa} = \pm\sqrt{\frac{\sigma_{xg}^2+\sigma_{xh}^2}{(2015.5-1991.25)^2}}$
$y0$	as	Difference in right ascension (primary – secondary) at time $t0$	$yg - ya(2015.5 - t0)$	$\sigma_{y0} = \pm\sqrt{\left[(2015.5 - t0)\sigma_{ya}\right]^2 + \sigma_{yg}^2}$
ya	as year^{-1}	Rate of change of right ascension	$(yg - yh)/(2015.5 - 1991.25)$	$\sigma_{ya} = \pm\sqrt{\frac{\sigma_{yg}^2+\sigma_{yh}^2}{(2015.5-1991.25)^2}}$
$t0$	year	Time $t0$	2000.0	$\sigma_{t0} = 0$
$\theta 0$	deg	Position angle of secondary relative to primary at time $t0$	$\frac{180}{\pi}\arctan 2(y0, x0)$	$\sigma_{\theta 0} = \pm\frac{180}{\pi}\sqrt{\frac{(x0\sigma_{y0})^2+(y0\sigma_{x0})^2}{(x0^2+y0^2)^2}}$
$\rho 0$	as	Separation of primary and secondary at time $t0$	$\sqrt{x0^2 + y0^2}$	$\sigma_{\rho 0} = \pm\sqrt{\frac{(x0\sigma_{x0})^2+(y0\sigma_{y0})^2}{x0^2+y0^2}}$

Note: Definitions and mathematical derivations of the Cartesian coordinates of the HIPPARCOS and *Gaia DR2* positions (xh,yh and xg,yg, respectively) and their uncertainties (σ_{xh},σ_{yh} and σ_{xg},σ_{yg}), respectively, are given in Appendices A and B, respectively.

TABLE 5 Formulae for calculating an ephemeris

Position	Units	Description	Definition	Uncertainty
x_{Eph}	as	Difference in declination (primary – secondary) at time t_{Eph}	$xa(t_{\mathrm{Eph}} - t0) + x0$	$\sigma_{x\mathrm{Eph}} = \pm\sqrt{\left[\left(t_{\mathrm{Eph}} - t0\right)\sigma_{xa}\right]^2 + \sigma_{x0}^2}$
y_{Eph}	as	Difference in right ascension (primary – secondary) at time t_{Eph}	$ya(t_{\mathrm{Eph}} - t0) + y0$	$\sigma_{y\mathrm{Eph}} = \pm\sqrt{\left[\left(t_{\mathrm{Eph}} - t0\right)\sigma_{ya}\right]^2 + \sigma_{y0}^2}$
θ_{Eph}	deg	Position angle of secondary relative to primary at time t_{Eph}	$\frac{180}{\pi}\arctan 2\left(y_{\mathrm{Eph}}, x_{\mathrm{Eph}}\right)$	$\sigma_{\theta\mathrm{Eph}} = \pm\frac{180}{\pi}\sqrt{\frac{\left(x_{\mathrm{Eph}}\sigma_{y_{\mathrm{Eph}}}\right)^2+\left(y_{\mathrm{Eph}}\sigma_{x_{\mathrm{Eph}}}\right)^2}{\left(x_{\mathrm{Eph}}^2+y_{\mathrm{Eph}}^2\right)^2}}$
ρ_{Eph}	as	Separation of primary and secondary at time t_{Eph}	$\sqrt{x_{\mathrm{Eph}}^2 + y_{\mathrm{Eph}}^2}$	$\sigma_{\rho\mathrm{Eph}} = \pm\sqrt{\frac{\left(x_{\mathrm{Eph}}\sigma_{x_{\mathrm{Eph}}}\right)^2+\left(y_{\mathrm{Eph}}\sigma_{y_{\mathrm{Eph}}}\right)^2}{x_{\mathrm{Eph}}^2+y_{\mathrm{Eph}}^2}}$

Note: t_{Eph} is the time in decimal years for which an ephemeris is required.

of 11 double stars in the *Working Dunlop Catalogue* also have entries in the SCORE (some of which could not be confirmed here as optical double stars), from which a comparison of rectilinear elements can be made, after the rectilinear elements from the SCORE have been converted to $T0 = 2000.0$. Table 6 lists the rectilinear elements taken directly from the SCORE (without conversion), and the rectilinear elements derived from the method proposed in this paper. Column 1 gives the catalogue number from the original *Dunlop Catalogue*, and column 2 gives the WDS system name and underneath the Discoverer Code. Columns 3–9 give the rectilinear elements from this paper and the corresponding ones from the SCORE.

The results of our comparison between our rectilinear elements and those from the SCORE on the test sample of 11 double stars in Table 6 are summarized in Table 7. Column 1 of Table 7 lists our rectilinear elements with the SCORE equivalents in brackets. Columns 2–5 give the number of each of our Rectilinear Element's uncertainty that falls within 1σ, 2σ, and 3σ, and greater than 3σ of the corresponding uncertainty from the SCORE, respectively.

We compared the rectilinear elements generated with those in the SCORE by:

- using the rectilinear elements of the 11 double stars in the SCORE to generate an ephemeris for $t_{\mathrm{Eph}} = 2000.0$ (necessary as our $\theta 0$ and $\rho 0$ are all at 2000.0 and the corresponding elements from the SCORE, THETA0 and RHO0 respectively, are at different epochs);
- recalling that our xa and ya are equivalent to YA and XA from the SCORE, respectively; and

TABLE 6 Test sample of rectilinear elements of 11 double stars from the *Working Dunlop Catalogue* that also have entries in the SCORE

No.	WDS Discoverer code	*x*0 (DE)″ +/− *Y*0 (DE)″ +/−	*xa*″/year +/− *YA*″/year +/−	*y*0 (RA)″ +/− *X*0 (RA)″ +/−	*ya*″/year +/− *XA*″/year +/−	*t*0 year *T*0 year	*θ*0° +/− THETA0° +/−	*ρ*0″ +/− RHO0″ +/−
27	06163-5913	−20.723058	0.107208	−27.500542	0.072198	2000.000	233.000	34.434
	DUN 27AB	0.000105	0.000006	0.000257	0.000017		0.000	0.000
		−22.026257	0.109352	−28.366165	0.071572	1987.755	232.170	35.914
		0.060615	0.002781	0.030768	0.001412		0.080	0.044
29	06291-4022	−30.146026	−0.026564	57.018287	−0.055537	2000.000	117.866	64.497
	DUN 29	0.000102	0.000006	0.000382	0.000025		0.000	0.000
		−29.801716	−0.027721	57.704216	−0.056859	1988.246	117.310	64.946
		0.054306	0.000944	0.037148	0.000646		0.050	0.041
151	13573-5602	21.095364	0.083706	29.543929	0.234760	2000.000	54.472	36.302
	DUN 151AB	0.000426	0.000016	0.000518	0.000032		0.001	0.000
		19.707088	0.083942	25.497437	0.234590	1982.651	52.300	32.226
		0.082986	0.001178	0.035395	0.000503		0.120	0.058
163	14380-5431	−14.686554	0.027036	62.645700	0.071106	2000.000	103.194	64.344
	DUN 163	0.000115	0.000006	0.000372	0.000024		0.000	0.000
		−15.076161	0.024868	61.561581	0.070268	1984.638	103.760	63.381
		0.057987	0.001004	0.037107	0.000643		0.050	0.039
178	15116-4517	−6.249198	−0.061738	−30.141038	0.049520	2000.000	258.287	30.782
	DUN 178AC	0.000104	0.000006	0.000453	0.000029		0.000	0.000
		−5.657417	−0.060943	−30.675056	0.048137	1989.454	259.550	31.192
		0.054860	0.001079	0.061269	0.001205		0.100	0.061
187	15336-4732	−19.271781	0.021731	−15.064421	0.064620	2000.000	218.014	24.461
	DUN 187	0.010378	0.000670	0.006532	0.000421		0.019	0.009
		−18.898331	−0.000165	−15.465071	0.074130	1996.419	219.290	24.420
		0.106683	0.002485	0.051082	0.001190		0.180	0.089
203	16331-6054	2.729017	0.103470	−22.019539	0.073548	2000.000	277.065	22.188
	DUN 203	0.000100	0.000006	0.009531	0.000615		0.003	0.009
		1.002347	0.101794	−23.280334	0.071153	1983.182	272.470	23.302
		0.053328	0.001080	0.065672	0.001330		0.130	0.066
214	17133-6712	36.329818	0.080494	8.998040	0.146916	2000.000	13.911	37.428
	DUN 214AB	0.003453	0.000223	0.002306	0.000149		0.004	0.003
		35.404930	0.079604	7.425738	0.151083	1988.470	11.850	36.175
		0.118374	0.002824	0.116790	0.002786		0.190	0.118
219	17589-3652	−14.413043	−0.057786	−51.139547	−0.035364	2000.000	254.260	53.132
	DUN 219AB	0.004029	0.000260	0.002339	0.000151		0.004	0.003
		−13.562767	−0.063280	−50.699947	−0.034422	1985.265	255.020	52.483
		0.106047	0.002934	0.053613	0.001483		0.110	0.059

TABLE 6 (Continued)

No.	WDS Discoverer code	$x0$ (DE)″ +/− $Y0$ (DE)″ +/−	xa″/year +/− YA″/year +/−	$y0$ (RA)″ +/− $X0$ (RA)″ +/−	ya″/year +/− XA″/year +/−	$t0$ year $T0$ year	$\theta 0$° +/− THETA0°	$\rho 0$″ +/− RHO0″ +/−
247	23180-6100	19.979530	0.099800	−45.932176	−0.056297	2000.000	293.508	50.089
	DUN 247	0.000099	0.000006	0.000243	0.000016		0.000	0.000
		19.307772	0.094191	−45.642963	−0.057577	1993.129	292.930	49.559
		0.064555	0.001424	0.088271	0.001947		0.080	0.085
250	23272-5017	3.564678	0.029713	28.124534	−0.128381	2000.000	82.776	28.350
	DUN 250	0.000102	0.000006	0.001902	0.000123		0.001	0.002
		3.304039	0.029910	29.239500	−0.127354	1991.423	83.550	29.426
		0.042141	0.000840	0.034182	0.000681		0.080	0.034

Note: The first set of elements ($x0$, xa, $y0$, ya, $t0$, $\theta 0$, $\rho 0$) are the result of the method proposed in this paper. For their definitions, see Table 4. The second set of elements ($Y0$, YA, $X0$, XA, $T0$, THETA0, RHO0) are those from the SCORE. Following the SCORE, the first four rectilinear elements are given to six decimal places.

TABLE 7 Comparison of rectilinear elements from Table 6 with those from SCORE at $t0 = 2000.0$

Rectilinear elements	$<1\sigma$	$<2\,\sigma$	$<3\sigma$	$>3\sigma$
$x0$ ($\equiv Y0$ of SCORE at 2000.0)	10	10	10	1
xa ($\equiv YA$ of SCORE at 2000.0)	5	8	9	2
$y0$ ($\equiv X0$ of SCORE at 2000.0)	7	10	11	0
ya ($\equiv XA$ of SCORE at 2000.0)	4	9	10	1
$\theta 0$ ($\equiv\theta 0$ of SCORE at 2000.0)	9	10	10	1
$\rho 0$ ($\equiv\rho 0$ of SCORE at 2000.0)	7	103	11	0
Overall	42 (64%)	57 (86%)	61 (92%)	5 (8%)

Note: See Section 3.1.

- then noting if our Rectilinear Element falls within 1σ, 2σ, 3σ, or beyond 3σ, of the Rectilinear Element generated by the SCORE at $t_{\mathrm{Eph}} = 2000.0$.

From Table 7, 86% of the comparison rectilinear elements fall within 2σ of the SCORE uncertainties, and our uncertainties are, on average, at least one order of magnitude smaller than those in the SCORE. In particular, our uncertainties for $\theta 0$ and $\rho 0$—the two most important parameters for a given epoch—are as little as 2 and 4%, respectively, of those from the SCORE. In addition, 4 out of 11 (36%) of our residuals (sum of distances between observed and calculated positions) are smaller than those generated from the SCORE (on residuals, see paper II). Assuming the sample of 11 is representative, then an order of 80–90% of our rectilinear elements would also fall within 2σ of the uncertainties of any Rectilinear Element generated from the SCORE.

4 | RESULTS AND DISCUSSION: RECTILINEAR ELEMENTS

The 14 sets of rectilinear elements of confirmed optical double stars from the *Working Dunlop Catalogue* (Table 1) are given in Table 8, and are recommended for inclusion in the SCORE. Column 1 (No.) contains the catalogue numbers from the original *Dunlop Catalogue*, and column 2 is the WDS identifier for the star system, underneath which is the Discoverer Code for the particular double star within that system. Columns 3–9 contain the rectilinear elements, underneath which are given the uncertainties from the method presented in this paper (Section 3).

Plots of the 14 optical double stars are given in Appendix C: rectilinear plots (Figures C1–C14). The primary is at 0.0 (represented by the large + sign) and the units on both axes are arcseconds. The thick black line represents the Rectilinear motion of the secondary

TABLE 8 Rectilinear elements of the 14 "confirmed" optical double stars from the *Working Dunlop Catalogue*

No.	WDS Discoverer code	$x0''$ (≡*YO*) +/−	xa''/yr (≡*YA*) +/−	$y0''$ (≡*XO*) +/−	ya''/year (≡*XA*) +/−	$t0$ year (≡*TO*) +/−	$\theta 0°$ (≡THETAO) +/−	$\rho 0''$ (≡RHO0) +/−
4	01388-5327	−2.587946	0.001093	10.006183	−0.001618	2000.000	104.501	10.335
	DUN 4	0.000098	0.000006	0.002479	0.000160		0.003	0.002
28	06240-3642	17.208936	−0.060040	61.278826	−0.012771	2000.000	74.314	63.649
	DUN 28AC	0.000123	0.000007	0.000366	0.000023		0.000	0.000
29	06291-4022	−30.146026	−0.026564	57.018287	−0.055537	2000.000	117.866	64.497
	DUN 29	0.000102	0.000006	0.000382	0.000025		0.000	0.000
40	07092-5622	−29.204218	−0.000046	22.335882	−0.009278	2000.000	142.591	36.767
	DUN 40	0.005786	0.000373	0.003331	0.000215		0.007	0.005
73	08562-5532	65.861664	0.000468	0.286351	0.022489	2000.000	0.249	65.862
	DUN 73AB	0.005306	0.000342	0.002650	0.000171		0.002	0.005
79	09336-4945	117.722013	0.033202	76.462160	0.054654	2000.000	33.004	140.374
	DUN 79	0.003389	0.000219	0.002040	0.000132		0.001	0.003
146	13493-4031	4.056898	−0.003984	66.703532	0.089333	2000.000	86.520	66.827
	DUN 146	0.003837	0.000247	0.002593	0.000167		0.003	0.003
155	14077-5341	18.360533	−0.015981	1.973034	−0.050425	2000.000	6.134	18.466
	DUN 155	0.000119	0.000006	0.004866	0.000314		0.015	0.001
178	15116-4517	−6.249198	−0.061738	−30.141038	0.049520	2000.000	258.287	30.782
	DUN 178AC	0.000104	0.000006	0.000453	0.000029		0.000	0.000
184	15263-4252	−2.705922	0.023630	20.961041	0.061352	2000.000	97.356	21.135
	DUN 184	0.000098	0.000006	0.007905	0.000510		0.003	0.008
200	16225-4355	−37.888038	0.014447	−10.111217	0.009853	2000.000	194.942	39.214
	DUN 200	0.013870	0.000895	0.012942	0.000835		0.019	0.014
225	19124-5148	−23.713882	−0.009434	−66.085579	0.000528	2000.000	250.260	70.211
	DUN 225AB	0.000124	0.000007	0.000509	0.000033		0.000	0.000
241	22366-3140	79.481567	0.036499	48.658853	0.033682	2000.000	31.475	93.193
	DUN 241	0.000140	0.000007	0.000470	0.000030		0.000	0.000
250	23272-5017	3.564678	0.029713	28.124534	−0.128381	2000.000	82.776	28.350
	DUN 250	0.000102	0.000006	0.001902	0.000123		0.001	0.002

Note: Following the practice of the SCORE, the first four rectilinear elements are given to six decimal places. $t0$ is exactly 2000.0. An explanation of the columns is given in Section 4.

compared with the primary as calculated in this paper. The line represents the relative proper motion of the secondary compared with the primary according to HIPPARCOS (via ASCC). The blue line represents the relative proper motion of the secondary compared with the primary according to *Gaia DR2*. In most of the plots, these three lines cannot be easily distinguished because of their similarity in magnitude and direction.

Individual unweighted historic measures for the period 1820–2020 are now plotted onto the HIPPARCOS/Gaia Rectilinear plot after precession to equinox 2000.0 and are color-coded, following Hartkopf & Mason (2020): green, blue, and purple, which indicate micrometric, interferometric, and photographic/CCD measures, respectively. A red "H" and "T" indicate HIPPARCOS and Tycho positions, respectively. A green "G" indicates the *Gaia DR2* position. Measures are connected to their predicted locations by dotted lines. A dotted line runs from the origin to the predicted relative position of the secondary at epoch 2000.0.

Overall, the mean uncertainty of the 14 positions at 2000.0 ($x0$,$y0$) is ∼3 mas and the mean uncertainty of the

calculated proper motions (*xa*,*ya*) is ∼2 mas year^{-1}. This compares with the SCORE (Section 1) of ∼200 mas and ∼3 mas year^{-1}, respectively.

5 | SUMMARY

We propose here a variant on the method of calculating rectilinear elements that differs from the currently accepted method by using (a) standard polar to Cartesian conversion; (b) only two high-precision space-based astrometric measures, that of HIPPARCOS (via ASCC) and *Gaia DR2*; and (c) fixing the *t*0 (*T*0) at precisely 2000.0 in every set of rectilinear elements.

With our test of rectilinear elements, the uncertainties were, on average, an order of magnitude smaller than those in the SCORE, and we expect ∼80% or higher of any rectilinear elements generated by our technique to fall within 2σ of the uncertainties of any rectilinear elements generated using the current method.

We stress that these results were obtained *without* the inclusion of historic non-space-based measures, and suggest that the inclusion of these measures (weighed or unweighted) adds little to the computation of rectilinear elements for optical double stars. However, ongoing follow-up with terrestrial-based high-precision measures to detect both the presence of perturbers and as a check on space-based astrometry may continue to be vital.

ACKNOWLEDGMENTS

This research has made use of: NASA's Astrophysics Data System, operated at CDS, Strasbourg, France. the SIMBAD database, operated at CDS, Strasbourg, France. The *Aladin sky atlas* developed at CDS, Strasbourg Observatory, France. The *Sixth Catalogue of Orbits of Visual Binary Stars* maintained by the United States Naval Observatory. The *Washington Double Star Catalogue* (WDS) maintained by the United States Naval Observatory. The *Second Catalogue of Rectilinear Elements* maintained by the United States Naval Observatory (SCORE). Open access publishing facilitated by University of Southern Queensland, as part of the Wiley - University of Southern Queensland agreement via the Council of Australian University Librarians.

ORCID

Roderick R. Letchford https://orcid.org/0000-0002-9753-9058

Graeme L. White https://orcid.org/0000-0002-4914-6292

Carolyn J. Brown https://orcid.org/0000-0001-6649-4531

REFERENCES

Debehogne, H., & de Freitas Mourao, R. R. 1977, *A&A*, *61*(4), 453.

Dunlop, J. 1829, *MNRAS*, *3*(1), 257.

Gaia Collaboration,Brown, A. G. A., Vallenari, A., et al. 2018, *A&A*, *616*, A1.

Hartkopf, W. I., & Mason, B. D. 2020, Second Catalog of Rectilinear Elements. Retrieved from http://www.astro.gsu.edu/wds/lin2.html.

Hartkopf, W. I., Mason, B. D., Finch, C. T., Zacharias, N., Wycoff, G. L., & Hsu, D. 2013, *AJ*, *146*(76), 1.

Hartkopf, W. I., Mason, B. D., & Worley, C. E. 2001, *AJ*, *122*(6), 3472.

Kharchenko, N. V. 2001, *KFNT*, *17*(5), 409.

Letchford, R. R., White, G. L., & Brown, C. J. 2022a, *MNRAS*, *510*, 5330.

Letchford, R. R., White, G. L., & Brown, C. J. 2022b, *Astron. Nachr*, *342*(3), 13.

Letchford, R. R., White, G. L., & Ernest, A. D. 2018, *JDSO*, *14*, 208.

Letchford, R. R., White, G. L., & Ernest, A. D. 2019, *JDSO*, *15*, 393.

Mason, B. D., Douglass, G. G., & Hartkopf, W. I. 1999, *AJ*, *117*(2), 1023.

Mason, B. D., Wycoff, G. L., Hartkopf, W. I., Douglass, G. G., & Worley, C. E. 2001, *AJ*, *122*(6), 3466.

Perryman, M. A. C., Lindegren, L., Kovalevsky, J., et al. 1997, *A&A*, *500*, 501.

Schlesinger, F., & Alter, D. 1912, *PAllO*, *2*, 13.

Torres, G. 1985, *A&AS*, *62*, 191.

Torres, G. 1988a, *A&AS*, *72*, 209.

Torres, G. 1988b, *Ap&SS*, *141*(2), 271.

AUTHOR BIOGRAPHY

Roderick R. Letchford is currently completing his Ph.D. in Astrophysics at the University of Southern Queensland. He teaches at Vianney College Seminary, Wagga Wagga NSW Australia.

How to cite this article: Letchford, R. R., White, G. L., & Brown, C. J. 2022, *Astron. Nachr.*, *343*, e220018. https://doi.org/10.1002/asna.20220018

APPENDIX A. CARTESIAN COORDINATES OF HIPPARCOS AND *GAIA DR2* POSITIONS

Here we present the following coordinates:

- *xh* = *x* Cartesian coordinate of the HIPPARCOS position relative to the primary, in arcseconds.
- *yh* = *y* Cartesian coordinate of the HIPPARCOS position relative to the primary, in arcseconds.
- θh = Polar coordinate of the HIPPARCOS position angle of the secondary relative the the primary, in degrees.

- ρh = Polar coordinate of the HIPPARCOS angular separation of the secondary from the primary, in arcseconds.

The procedure is the same for *Gaia DR2* coordinates, xg, yg, and θg, ρg, respectively.
Let:

- RA1h = Right ascension of primary from HIPPARCOS at equinox 2000.0 (≡ ICRS) and epoch 1991.25, measured in degrees.
- DE1h = Declination of primary from HIPPARCOS at equinox 2000.0 and epoch 1991.25, measured in degrees.
- RA2h = Right ascension of secondary from HIPPARCOS at equinox 2000.0 and epoch 1991.25, measured in degrees.
- DE2h = Declination of secondary from HIPPARCOS at equinox 2000.0 and epoch 1991.25, measured in degrees.

Therefore:

$$yh'' = 3600(\text{RA2h} - \text{RA1h})\cos(\text{DE1h})$$
$$xh'' = 3600(\text{DE2h} - \text{DE1h}).$$

And so:

$$\theta h^{\circ} = \begin{cases} \frac{180}{\pi}\arctan 2(yh, xh) \\ \theta h + 360, \text{if } \theta h < 0 \\ \theta h - 360, \text{if } \theta h > 360 \end{cases}$$
$$\rho h'' = \sqrt{xh^2 + yh^2}.$$

The definition of arctan2 (from paper II) is:

$$\arctan 2(Q, R) = \begin{cases} \arctan(Q/R), \text{if } R > Q \\ \frac{\pi}{2} - \arctan(Q/R), \text{if } Q > 0 \\ -\frac{\pi}{2} - \arctan(Q/R), \text{if } Q < 0 \\ \arctan(Q/R) \pm \pi, \text{if } R < 0 \\ \text{undefined, if } R = 0 \text{ and } Q = 0 \end{cases} . \quad \text{(A1)}$$

APPENDIX B. UNCERTAINTIES OF THE CARTESIAN COORDINATES OF HIPPARCOS AND *GAIA DR2* POSITIONS

Here we derive the following uncertainties:

- σ_{xh} = uncertainty in xh, in arcseconds.
- σ_{yh} = uncertainty in yh, in arcseconds.

Again the procedure is the same for *Gaia DR2* uncertainties, σ_{xg} and σ_{yg}.

Throughout, the definition of uncertainties is that of:

$$\sigma_{f(x_i)} = \pm\sqrt{\sum\left(\frac{\partial f(x_i)}{\partial x_i}\sigma_{x_i}\right)^2}, \quad \text{(B2)}$$

where σ_{xi} is the uncertainty of an individual x_i.

Let:

- RAh1e = uncertainty (error) in right ascension of the primary from HIPPARCOS at equinox 2000.0 (≡ ICRS) and epoch 1991.25, measured in arcseconds.
- RAh2e = uncertainty (error) in right ascension of the secondary from HIPPARCOS at equinox 2000.0 and epoch 1991.25, measured in arcseconds.
- DEh1e = uncertainty (error) in declination of the primary from HIPPARCOS at equinox 2000.0 and epoch 1991.25, measured in arcseconds.
- DEh2e = uncertainty (error) in declination of the secondary from HIPPARCOS at equinox 2000.0 and epoch 1991.25, measured in arcseconds.

Therefore:

$$\sigma_{yh} = \pm\sqrt{\begin{array}{c}\cos(\text{DEh1})^2\left(\text{RAh1}e^2 + \text{RAh2}e^2\right) \\ +\sin(\text{DEh1})^2(\text{RAh2} - \text{RAh1})^2\text{DEh1}e^2\end{array}}$$
$$\sigma_{xh} = \pm\sqrt{\text{DEh2}e^2 + \text{DEh1}e^2}.$$

The uncertainties of the polar coordinates:

$$\sigma_{\theta h}^{\circ} = \pm\frac{180}{\pi}\sqrt{\frac{(yh\sigma_{xh})^2 + (xh\sigma_{yh})^2}{(xh^2 + yh^2)^2}}$$
$$\sigma_{\rho h}'' = \pm\sqrt{\frac{(xh\sigma_{xh})^2 + (yh\sigma_{yh})^2}{xh^2 + yh^2}}.$$

APPENDIX C. RECTILINEAR PLOTS

A total of 40 double stars from the *Working Dunlop Catalogue* had sufficient *Gaia DR2* data for their binding energies to be calculated. Of those 40, a total of 14 were confirmed as optical double stars. For an explanation of the plots, see Section 4.

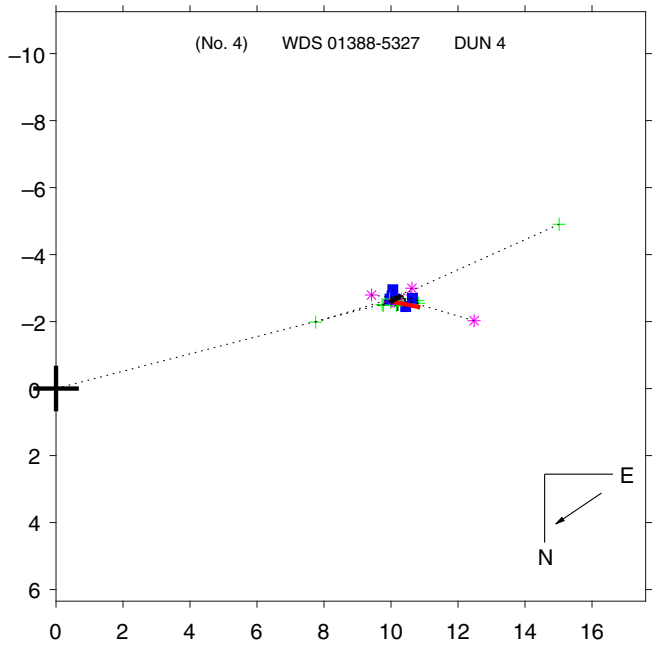

FIGURE C1 01388-5327 DUN 4

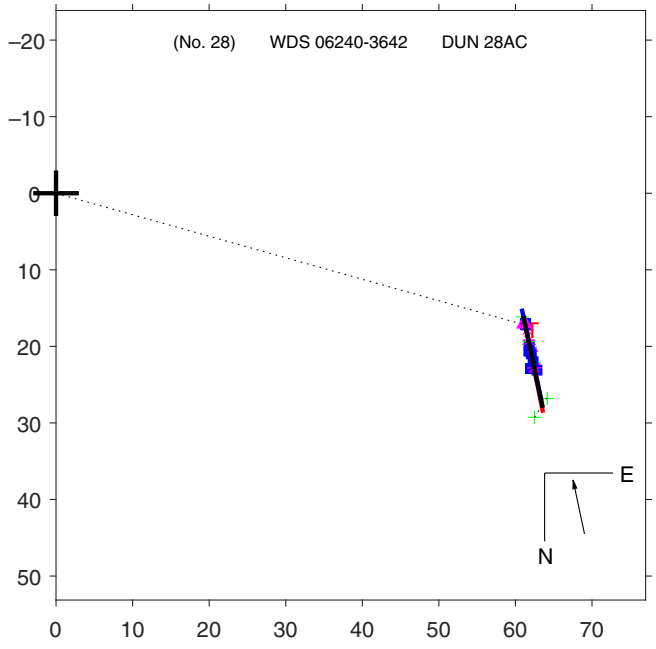

FIGURE C2 06240-3642 DUN 28AC

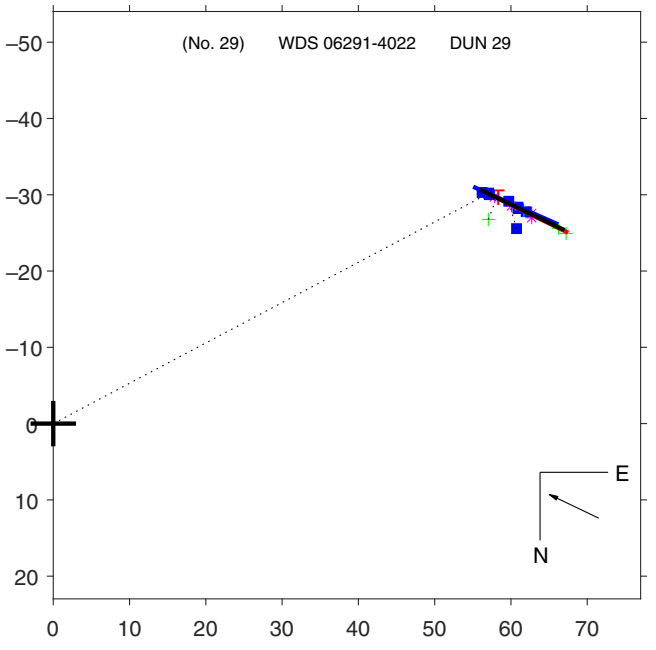

FIGURE C3 06291-4022 DUN 29

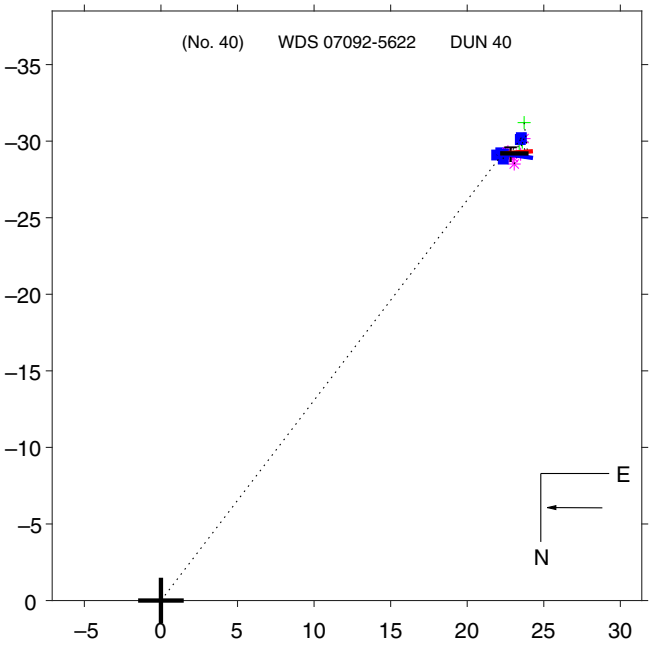

FIGURE C4 07092-5622 DUN 40

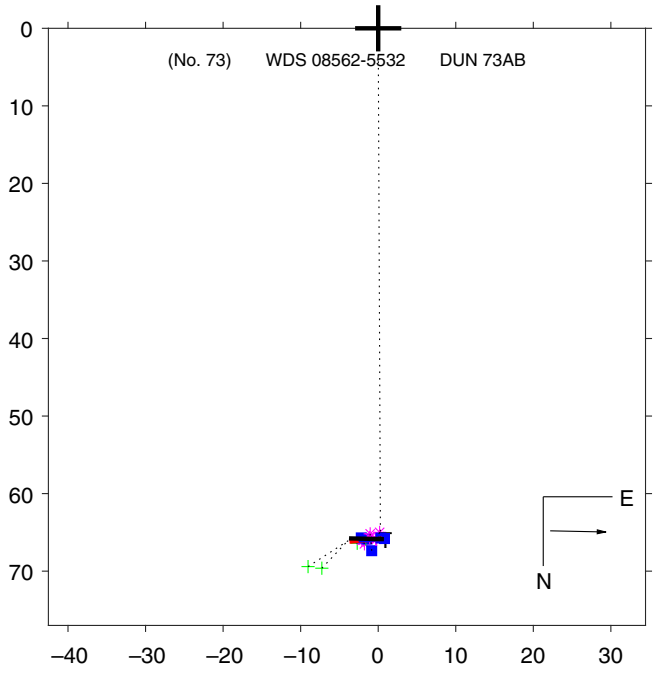

FIGURE C5 08562-5532 DUN 73AB

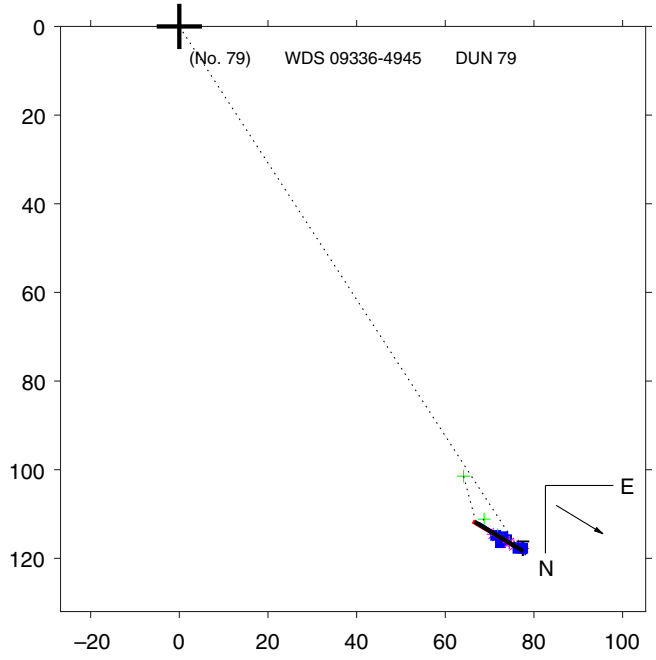

FIGURE C6 09336-4945 DUN 79

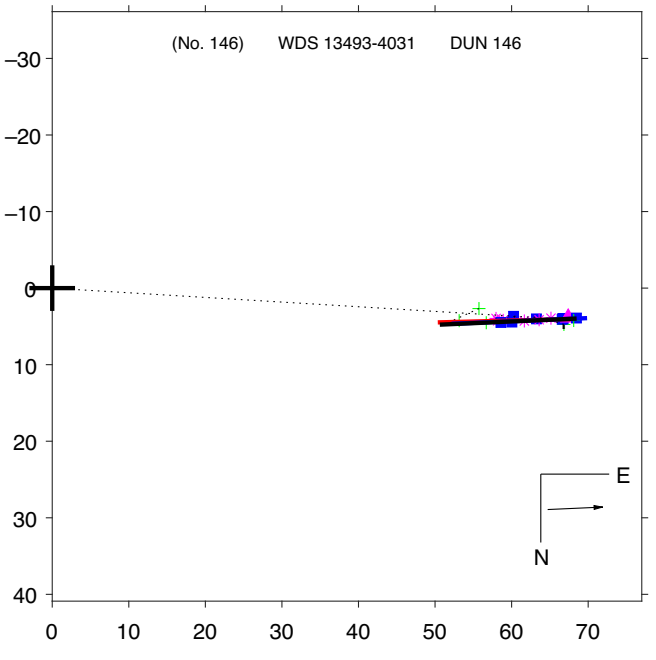

FIGURE C7 13493-4031 DUN 146

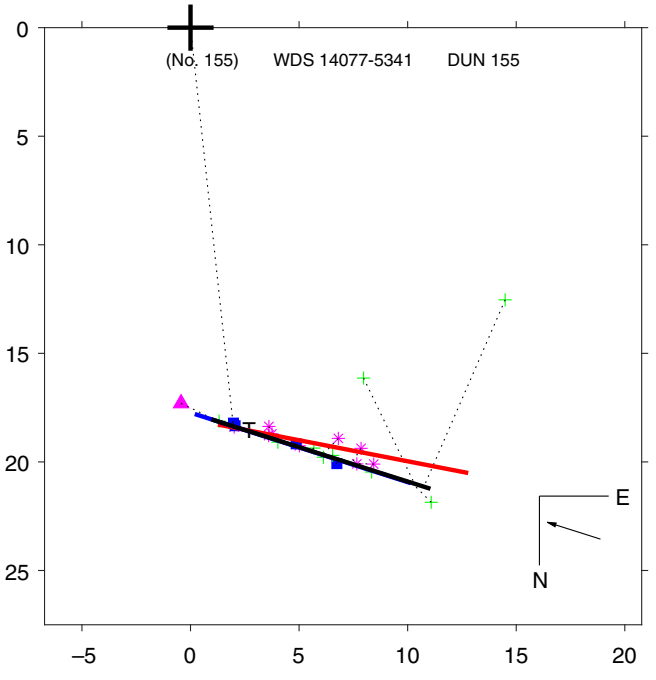

FIGURE C8 14077-5341 DUN 155

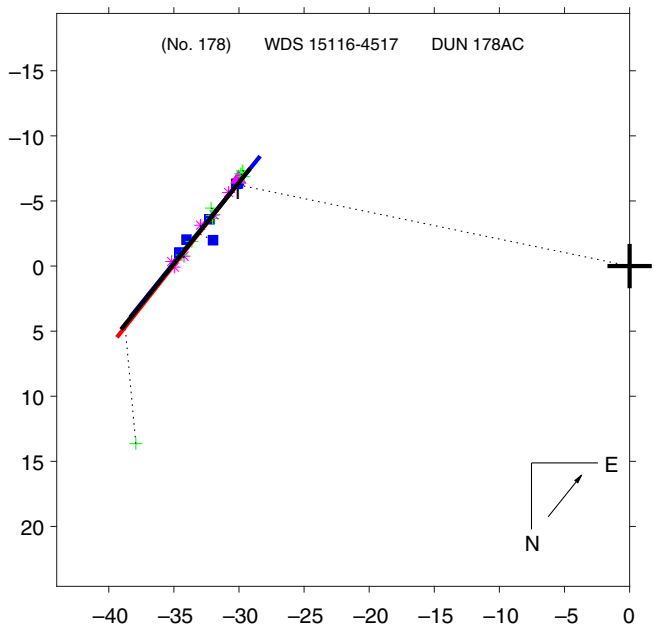

FIGURE C9 15116-4517 DUN 178AC

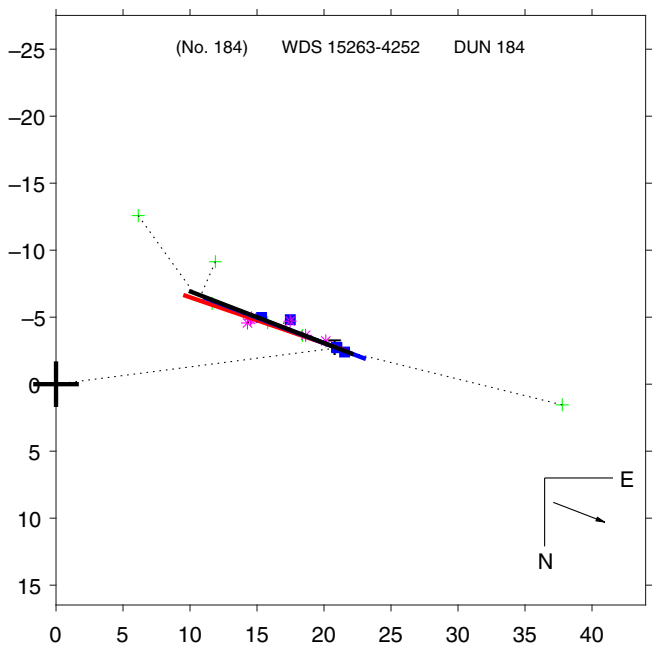

FIGURE C10 15263-4252 DUN 184

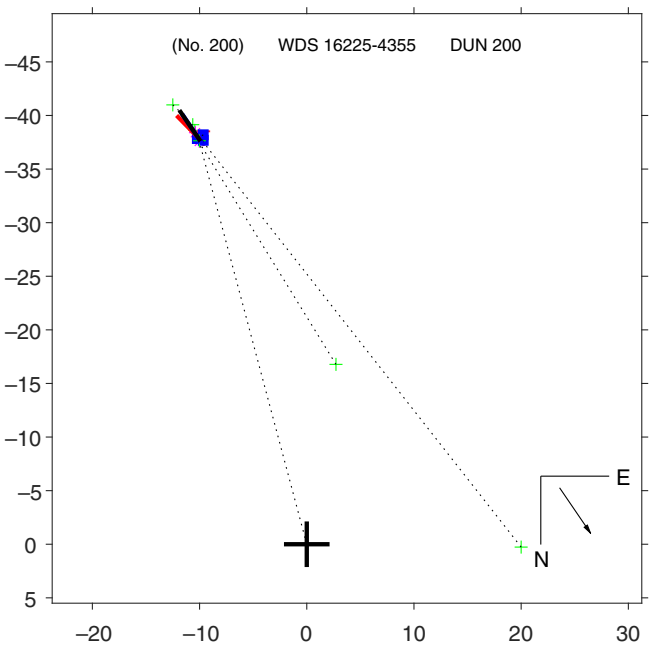

FIGURE C11 16225-4355 DUN 200

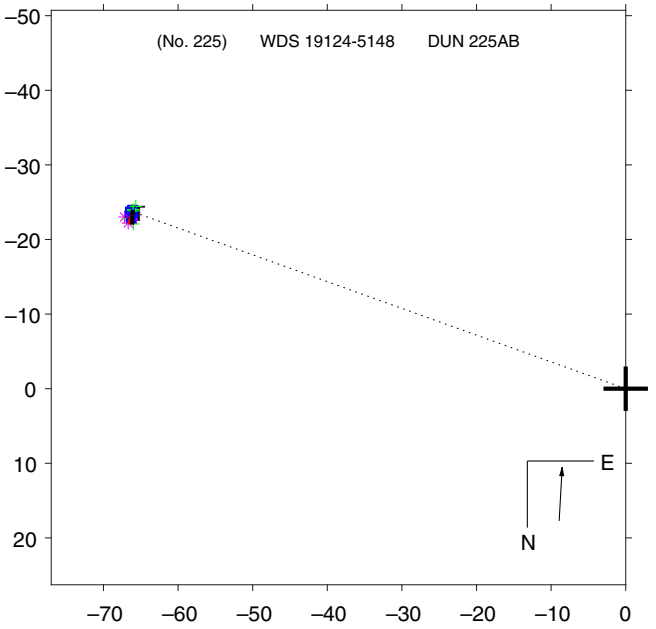

FIGURE C12 19124-5148 DUN 225AB

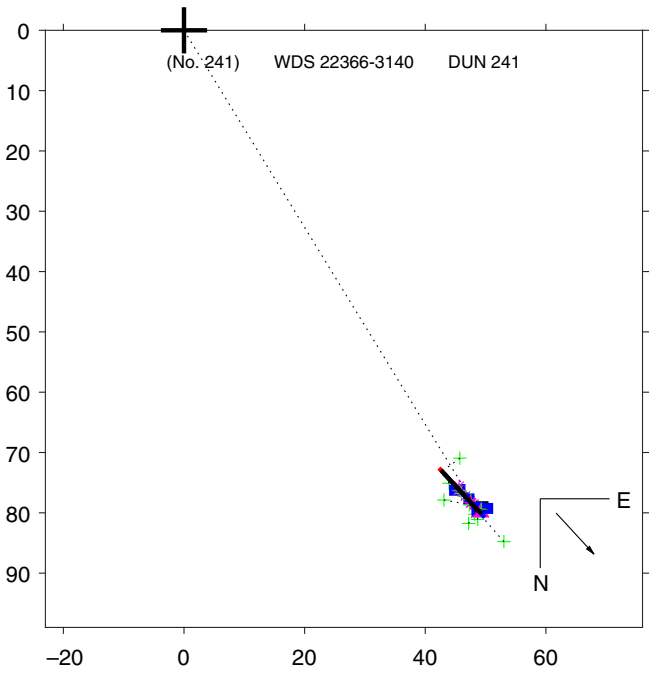

FIGURE C13 22366-3140 DUN 241

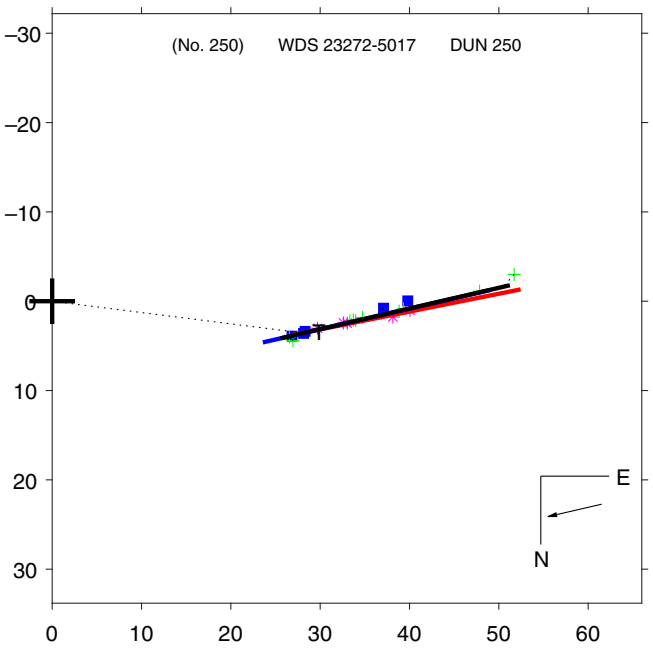

FIGURE C14 23272-5017 DUN 250